Serviceability behavior of High Strength Concrete I-beams reinforced with Carbon Fiber Reinforced Polymer bars

By
Assist. Prof. Dr.AbdulMuttalib I. Said, University of Baghdad, abdmusawi@yahoo.com
Oday Mohammed Abbas, Kufah University, auday_3d@yahoo.com

ABSTRACT

Fiber Reinforced Polymer (FRP) bars are anisotropic in nature and have high tensile strength in the fiber direction. The use of High-Strength Concrete (HSC) allows for better use of the high-strength properties of FRP bars. The mechanical properties of FRP bars can yield to large crack widths and deflections. As a result, the design of concrete elements reinforced with FRP materials is often governed by the Serviceability Limit States (SLS). This study investigates the short-term serviceability behavior of FRP RC I-beams. Eight RC I-beams reinforced with carbon-FRP (CFRP) and four steel RC I-beams, for comparison purposes, were tested under two-point loading. Deformations on the concrete and crack widths and spacing are measured and analyzed. A discussion on the main aspects of the SLS of FRP RC is introduced. The service load that fulfills the serviceability requirements, at a cross-section level, ranges between 0.27 and 0.38 times the ultimate load for sections dimensioned to fail in concrete crushing. The determinant criterion is the deflection limitation.

KEYWORDS: Fiber Reinforced Polymer, High-Strength Concrete, Serviceability.

سلوك حد الخدمة للعتبات الخرسانية عالية المقاومة ذات المقطع I والمسلحة بقضبان البوليمرات المسلحة بالألياف الكربونية

أ.م.د. عبد المطلب عيسى سعيد
م.م. عدي محمد عباس

الخلاصة

البوليمرات المسلحة بالألياف (FRP) في طبيعتها متباينة الخواص في الاتجاهات المختلفة وتملك قوة شد عالية باتجاه الالياف. أن استخدام الخرسانة عالية المقاومة (HSC) مع قضبان البوليمرات المسلحة بالألياف يسمح بالاستفادة القصوى من مقاومة الشد العالية لقضبان البوليمرات المسلحة بالألياف. أن الخواص الميكانيكية لقضبان البوليمرات المسلحة بالألياف قد تؤدي الى تشققات عريضة وهطول كبير. وكنتيجة لذلك، فان تصميم العناصر الخرسانية المسلحة بمواد البوليمرات المسلحة بالألياف غالبا ما تتحكم بها حالات حد الخدمة (SLS). هذه الدراسة تبحث في سلوك العتبات الخرسانية المشفه والمسلحة بقضبان البوليمرات المسلحة بالألياف ولحد الخدمة القصير الامد. تم فحص ثمانية عتبات خرسانية مشفه مسلحة بقضبان البوليمرات المسلحة بالألياف الكربونية واربعة عتبات خرسانية مشفه مسلحة بحديد التسليح لغرض المقارنة، تحت نقطتين للتحميل. التشوهات في الخرسانة وعرض التشققات والمسافات بينها تم قياسها و تحليلها. تم عرض دراسة حول اهم سمات حالة حد الخدمة (SLS) للعناصر المسلحة بالبوليمرات المسلحة بالألياف. ان اقصى حمل يلبي متطلبات حد الخدمة يتراوح بين 0.27 و 0.38 قيمة حمل الفشل العملي بالنسبة للنماذج المصممة لتفشل بتهشم الخرسانة. ان المحدد السائد كان محدد الهطول.

الكلمات الرئيسية: البوليمرات المسلحة بالألياف، الخرسانة عالية المقاومة، حد الخدمة.

1. INTRODUCTION

Recently, composite materials made of fibers embedded in a polymeric resin, also known as FRPs, have become an alternative to steel reinforcement for concrete structures. Because FRP materials are nonmagnetic and noncorrosive, the problems of electromagnetic interference and steel corrosion can be avoided with FRP reinforcement.

The most common types of fibers used in advanced composites for structural applications are the glass (GFRP), aramid (AFRP), and carbon (CFRP). The GFRP is the least expensive but has lower strength and significantly lower stiffness compared to other alternatives. CFRP is the stiffest, most durable, and the most expensive one. In the U.S., use of GFRP bars in MRI hospital room additions is becoming commonplace. Other applications, such as waterfront construction, top mat reinforcing for bridge decks, various precast applications, and ornamental and architectural concrete, are also becoming more frequent (Raffaello, Fico 2008).

When FRP bars are used, different structural behavior is expected due to their different mechanical and bond properties compared with those of steel rebars, in particular, their relatively low modulus of elasticity and their linear stress-strain behavior until failure. The lower stiffness of FRP bars can yield to large strains being mobilized in the bars at low levels of external loads and lead to large crack widths and deflections. As a result, the design of concrete elements reinforced with FRP materials is often governed by the serviceability limit states (SLS) (Nanni 2003). In addition, FRPs may exhibit significant creep rupture (or static fatigue) and fail under sustained loads at stresses lower than their tensile short-term strength (ACI Committee 440 2006, fib 2007).

In the last two decades, a number of studies were carried out to investigate the flexural response of FRP RC beams. Most of them show a limited number of experimental results and comparisons that often arrive at proposals for modifications of existing design procedures.

In the case of serviceability, and specifically for deflections of FRP RC elements, several authors propose coefficients to modify Branson's equation used in steel design codes (ACI Committee 318 2005), whereas other researchers suggest a modified equivalent moment of inertia derived from the integration of curvatures along the beam. These different approaches have been adopted in the various design guideline proposals for FRP RC (ISIS Canada 2001, CAN/CSA 2002, ACI Committee 440 2006, fib 2007).

For the case of cracking behavior of FRP RC elements, design equations and prediction models are generally based on similar formulation to that of steel RC, with coefficients that depend on the different characteristics of the rebars and their interaction with concrete. The design formulation for crack width, however, is still under discussion even for steel RC (Beeby 2004).

2. RESEARCH SIGNIFICANCE

This study aims at investigating the serviceability behavior of FRP RC I-beams, both experimentally and analytically, taking into account the contribution of the most important aspects of their flexural behavior.

3. TEST SPECIMENS

A total of twelve beams divided into three test groups (SB, CFB, and DCFB group), were fabricated and tested under static loading conditions to determine the different limit state behavior including ultimate and mode of failure of HSC I-beams see (**Fig. 1)**. Each of the beams was instrumented with external strain gauges to measure strain at different level of beams height. To measure crack widths, an optical micrometer with an accuracy of 0.02 mm was used. In order to measure the deflection of the tested beams, a minimum of three vertical dial gauges were used: one at the mid-span section, and two more vertical

dial gauges were added at the shear span, at 525 mm from the supports, see (**Fig. 2**).

The total length of each beam was $2440\ mm$, with an I cross-section of $b_f = 150\ mm$ (top and bottom flange width); $H = 300\ mm$ (overall height); $b_w = 90\ mm$ (width of the web); $h_f = 40\ mm$ (top flange thickness); $h_{fb} = 50\ mm$ (bottom flange thickness). The specimens were tested under two-point loading, with 2100 mm total span, and 800 mm shear span, the distance between loads being 500 mm, see (**Fig.3)**.

The beam types were identified using two terms. The first term, alphabetic term, of the identification corresponded to a beam group. SB for beam group of steel rebars, CFB for beam group of CFRP rebars, and DCFB for beam group of double reinforced CFRP rebars. The 'D' letter of the beam notation stands for the double reinforcements. The 'CF' or 'S' letters identify the type of longitudinal reinforcement: 'CF' for CFRP rbars and 'S' for steel rebars. The 'B' letter refers to the type of the structural element, (Beam element). The second term, numerical term, represent beam series. For each beam group, beams of series 1 were designed to have a similar load-carrying capacity of approximately P=100 kN; while, beams of series 2,3, and 4 were designed to have load carrying capacities of approximately 130 kN, 150 kN, and 165 kN, respectively.

It should be noted that, to satisfy serviceability requirements, the used design approach leads to different service loads for the test specimens as will be explained later. The target concrete strength for all test specimens was 50 MPa. The shear span was reinforced with an amount of steel stirrups enough to avoid shear failure. The geometric characteristics of the different sections are summarized in **Table 1** and (**Fig. 4**).

Three different trial mixes were prepared. The first one, without silica fume, obtained from local expert and the second one extracted from Table 7.2 of ACI234R-96 which was the MP1 mix. The third trial mix was designed using the step-by-step procedure of Silica Fume Association 2005. An increase in the cementitious materials and reduction in the *w/cm* ratio were carried out to mixture proportions of trial mix 3, and this lead to new trial mix (Trial mix 4). Trail mix 4 was also designed with the requirements of Silica Fume Association 2005. The mixture proportions and tested concrete cylinder results are listed in **Table-2.**

Beam specimens were cast in the postgraduate laboratory of Kufa University. In an attempt to produce concrete batches as similar as possible, a rigorous quality control was enforced on the production of concrete. For each group of specimens 10 cylinders, 3 cubes, and 3 prisms were cast, cured, and tested at the same time with the I-beam specimens. The first two cylinders were tested in compression at different concrete ages to ensure that the target compressive strength was achieved. Then, 4 of the cylinders were tested in compression. Three of them were tested in tension (splitting test). One of them was tested to determine the modulus of elasticity.

The compressive strength was determined according to ASTM C39 standard. The test results and average values of compressive strength were calculated as shown in **Table 3**. The concrete tensile strength was determined by splitting tensile tests on cylindrical specimens and by the flexural tensile strength of prismatic specimens. **Table 4** summarizes the experimental values for the tensile strength.

Three of the cylindrical specimens that were tested in compression were previously instrumented with strain gauges, see (**Fig. 5**). This configuration allowed to register the ascending branch of the stress-strain curve, as well as the concrete strain corresponding to the compressive strength. Cylinders 1, 2, and 3 were extracted from the cylindrical specimens of Group SB, CFB, and DCFB respectively. The stress-strain curves of the three cylinders are shown in (**Fig. 6**).

4. TEST PROCEDURE

All I-beam specimens were tested under a static two-point load test. A hydraulic jack with a capacity of 2000 kN was used to apply the load to the test beam through a spreader steel beam. The load was applied in load control mode at a load rate of 4 kN/min, and the strain gauges data were collected by a data acquisition system. The test was stopped every 5 kN to register the evolution of cracks, strains and the deflections along the beam. The crack pattern was drawn on the front face of the beam to make easy the positioning and identification of cracks during and after the test. The test setup is shown in (**Fig. 7**).

5. TEST RESULTS AND DISCUSSION

5.1. General Behavior and Crack Patterns

The CFB1 and DCFB1 failed by the rupturing of the CFRP rebars followed by concrete crushing. The CFRP rebars rupture can be recognized by the loud voice of fibers rupturing before failure. The other CFRP bar reinforced specimens failed by the crushing of concrete. The steel RC beams, (SB group), failed by yielding of the bars followed by concrete crushing. . **Table 5** summarizes the experimental load capacities (P_{exp}) for all 12 tested beams. The load capacity of the experimental beams increases with the reinforcement ratio. The cracking patterns were documented along the whole length of the beams at the different load steps. (**Fig. 8**) Shows a typical crack pattern for CFB1.

5.2 Experimental service load for the SLS of stresses in materials

By examining the data from strain gauges, additional information about the stresses in materials in the serviceability range can be obtained. The compressive stress in the concrete is usually limited at the service load in order to avoid longitudinal cracks, micro-cracks or high levels of creep, where they could result in unacceptable effects on the function of the structure (CEN 2004). According to Eurocode2, to avoid longitudinal cracks, the compressive stress in concrete is limited to $0.6f_c'$ under the characteristic combination of loads. In **Table 6**, the experimental load at which the concrete reaches this limit is registered, taking into account the experimental compressive strength f_c' (**Table 3**), the experimental stress strain curves (**Fig. 6**) and the experimental failure load P_{exp} (**Table 5**). The corresponding tensile stress in the reinforcement calculated form strain compatibility using the experimental reading of the first top two strain gauges is also shown.

For CFRP bar reinforced beams, results in **Table 6** shows that at a load of about 51% (3% deviation) of the experimental failure load, the concrete stress reaches the indicated limit to avoid longitudinal cracking ($\sigma_c = 0.6\, f_c'$). This percentage is low compared to this of the conventional steel RC beam 73% (9%), which corroborates the assumption that for this type of beams, high stresses are developed in the concrete at already early stages of loading.
For the ranges of loading corresponding to $\sigma_c = 0.6\, f_c'$, the tensile rebar stress varies between 37% (for CFB4) and 66% (for CFB1) of its nominal tensile strength f_{fu}. ACI 440.1R-06 would limit the stress of the CFRP bar to $0.55f_{fu}$, in which case, beams CFB1 and DCFB1, designed to fail in CFRP rebar rupture, would reach this limit before the concrete stress reaches $\sigma_c = 0.6\, f_c'$.

5.3 Load-midspan deflection

Comparing the experimental curves (**Figs. 9, 10,11 and 12**), larger deformations are obtained for lower reinforcement ratios, and vice versa. According to codes of practice, the deformation of a member shall not be such that it adversely affects its proper functioning or appearance. In Eurocode2, the sag of the element is limited to *l/250* and in ACI 440.1R-06, the service deflection limit of *l/240* under total service load is stated. **Table 7** summarizes the experimental load at which the instantaneous midspan total

deflection of the beam reaches *l/240*.
For CFB and DCFB group of tested beams, the instantaneous deflection of the beams reaches $l/240$ at an average load ratio of 31.6% (3.5% deviation) of the ultimate load. This mean value is lower than the one obtained for the control of stresses (51% of P_{exp}). It is therefore observed that the percentage of service load for CFRP RC is again much lower than for the steel RC beam (in this study, 73% P_{exp} with 3% deviation), showing the importance of the SLS when designing CFRP RC elements.

5.4 Experimental load for the SLS of cracking

(**Figs. 13,14,15 and 16**) show the evolutions of the crack width, of the first appeared crack, in the flexural zone measured with the optical micrometer, at lower point of tested I-beam height. Following ACI 440.1R-06 and CAN/CSA-S806, the crack width for the FRP RC experimental beams is generally limited to 0.5 to 0.7 mm. **Table 8** summarizes the resulting load at which the maximum crack width arrives to 0.7 mm for each beam tested. Following ACI 318M-08, the crack width for the steel RC experimental beams is generally limited to 0.4 mm. There is a doubt about the value of $P_{s,c}$ for DCFB3, and this is may be due to that the maximum experimental crack width didn't lie with the measured crack width.

For CFB and DCFB group of tested beams the maximum crack width reaches the value of 0.7 mm at a load of about 61% (32% deviation) the experimental failure load. This mean value results higher than the previously obtained in the study of the SLS for stresses in materials (58% of P_{exp}) and in the control of deflections (32% of P_{exp}). For the case of the steel RC beam, the ratio of experimental failure load is 100%, higher than the mean value of the CFRP RC beams.

6. SUMMARY AND CONCLUSIONS

Based on the findings of the previous sections, the governing parameters for the SLS are those limitations that are attained at the lowest value of load. The studied SLS are:

1. Stresses on materials limitation: the concrete compressive stress is limited to 60% the compressive strength f'_c, and the CFRP rebar tensile stress is limited to $0.55f_{fu}$. The service load is the load at which the maximum concrete compressive strain (read by the first top strain gauge) measures:

$$\varepsilon_c = 0.6\frac{f'_c}{E_c} \quad (1)$$

2. Crack width limitation: the maximum crack width is limited to 0.5-0.7 mm. The service load is the load at which the maximum value of crack width (measured at the central zone at the lower point of the section height) equals to:

$$w_{max} = 0.7\ \text{mm} \quad (2)$$

3. Deflection limitation: the deflection is limited to $L/240$. The service load is the load at which the instantaneous experimental midspan deflection (read by the vertical dial gauge) is:

$$\delta_{midspan} = \frac{L}{240} \quad (3)$$

The obtained service load P_s for each SLS is related to the experimental failure load P_{exp} for comparison purposes, and it is represented in (**Fig. 17**) and **Table 9**.

It is observed that for only CFB1 of the tested specimens, the SLS of cracking results is the restrictive limitation. The determinant criterion is the deflection limitation. The maximum crack width limitation presents the most scattered results, probably owing to the high variability of the maximum crack width parameter. The deflection limitation usually refers to the long-term deflection rather than the instantaneous one. In this study, since experimental values for the long-term deflection were not available, the instantaneous deflection was considered instead,

and consequently the maximum load causing deflections to reach these limiting values would be lower than that presented in the figures. Hence, the design under the SLS would probably be determined by the deflection limitation for these beams.

The most relevant conclusions of the present work can be summarized as follows:

1. Limiting compressive stress in concrete to $\sigma_c = 0.6\, f'_c$ gives somehow restrictive values for the maximum service moment to be attained at a section under the quasi-permanent loading condition. For the tested I-beams reinforced by CFRP rebars, this service moment would range between 1.8 and 4.2 times the cracking moment.

2. The tensile stress in the reinforcement is limited to avoid creep rupture. This limitation highly depends on the rebar properties, the environmental conditions and the loading period. Limiting the stress in the FRP bar generally leads to less restrictive situations than limiting the concrete stress, especially for beams design for concrete crushing failure mode.

3. Comparing the two serviceability limitations at a cross-section level (namely stresses in concrete and maximum crack width), it was observed that for lightly RC sections, the crack width limitation results more restrictive than the stresses in concrete, however, for sections with higher amounts of reinforcement, the predominant restriction is the concrete compressive stress.

4. Moreover, the service load that fulfills the serviceability requirements at a cross-section level ranges between 0.27 and 0.38 times the ultimate load for sections dimensioned to fail in concrete crushing. The determinant criterion is the deflection limitation.

REFERENCES

ACI 234R-96 (2000), "**Guide for the Use of Silica Fume in Concrete**", American Concrete Institute.

ACI Committee 318. (1995). "**ACI 318-95. Building code requirements for structural concrete (ACI 318-95) and commentary (ACI 318R-95).**" American Concrete Institute.

ACI Committee 440. (2006). "**ACI 440.1R-06. Guide for the design and construction of concrete reinforced with FRP bars.**" American Concrete Institute.

Beeby, A. W. (2004). "**The influence of the parameter φ/ρeff on crack widths.**" Structural Concrete, 5(2), 71-83.

CAN/CSA. (2002). "**CAN/CSA-S806. Design and construction of building components with fibre-reinforced polymers.**" Canadian Standards Association, Ontario, Canada, 177pp.

CEN. (2004). "**Eurocode 2: Design of concrete structures - Part 1.1: General rules and rules for buildings (EN 1992-1-1:2004).**" Comité Europeen De Normalisation, Brussels.

fib. (2007). "**FRP reinforcement in RC structures.**" Féderation International Du Béton, Fib Task Group 9.3, Fib Bulletin 40, Lausanne, witzerland, September 2007, 147pp.

ISIS Canada. (2001). "**Reinforcing concrete structures with fibre reinforced polymers – Design manual No. 3.**" ISIS Canada Corporation. University of Manitoba, Manitoba, Canada, 158pp.

Nanni, A. (2003). "**North American design guidelines for concrete reinforcement and strengthening using FRP: Principles, applications and unresolved issues.**" Construction and Building Materials, 17(6-7), 439-446.

Raffaello, Fico (2008)," **Limit States Design of Concrete Structures Reinforced with FRP Bars**", Ph.D. thesis, University of Naples Federico II.

Silica Fume Association, 2005, "**Silica Fume User's Manual,**" Publication No. FHWA-IF-05-016, Federal Highway Administration, Washington, DC.

Fig. 1 Twelve tested I-beams with concrete cylinders, cubes, and prisms.

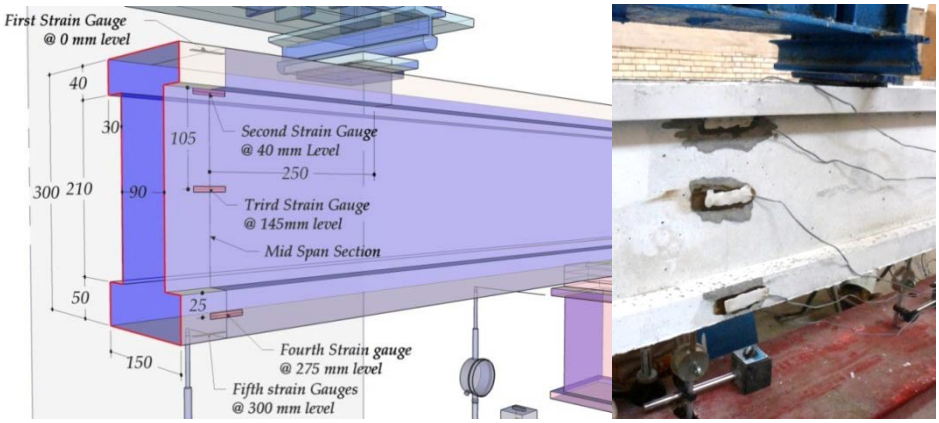

Fig. 2 strain gauges on the concrete surface of the midspan section

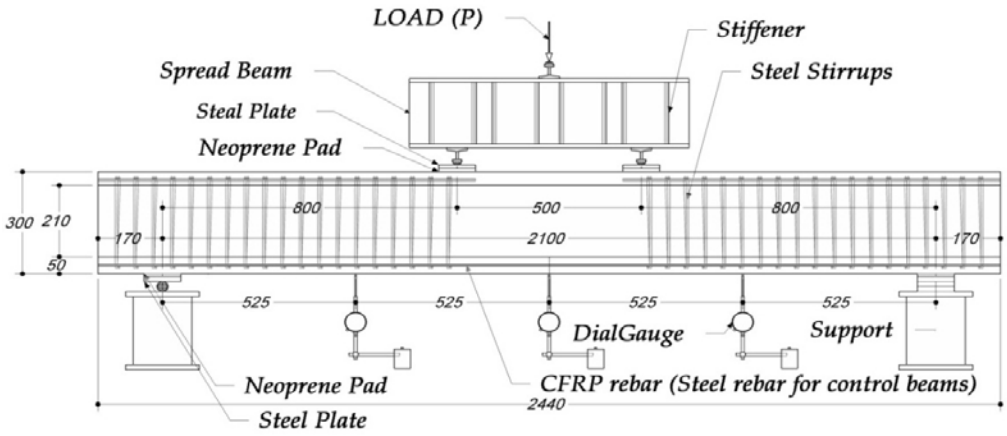

Fig. 3 Beam tests layout and internal reinforcement details.

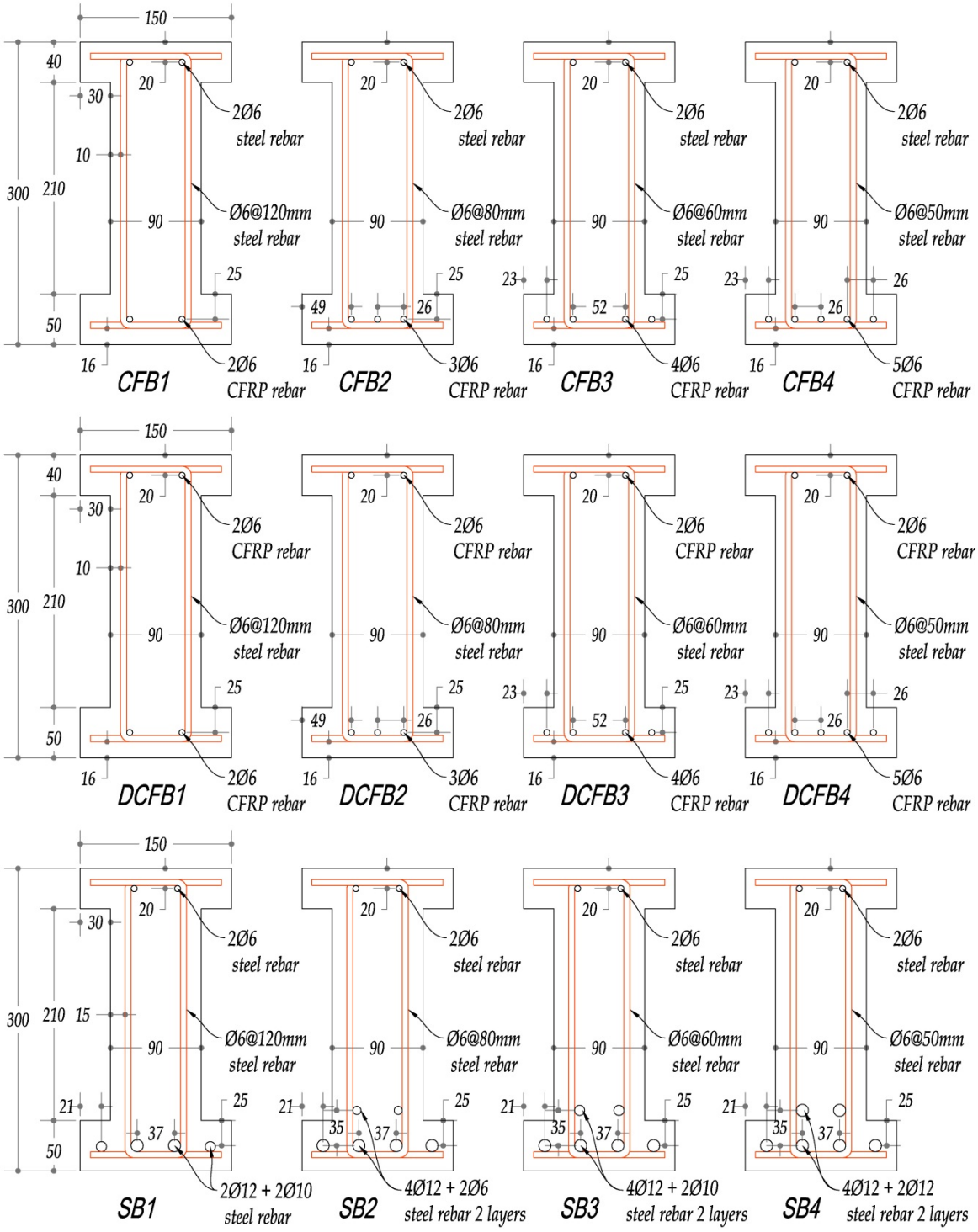

Fig. 4 Geometric characteristics of specimen sections (Section at shear span).

Table 1 Geometric characteristics of the sections of the tested beams.

Beam Designation	Ratio of A_r/A_{rb}*	Main Bottom Reinf. (A_r mm^2)	Type of rebar	Effective depth d (mm)	Top Reinf. (A'_r mm^2)	Type of rebar	Effective depth d' (mm)	Steel Stirrup for Shear span
CFB1	**0.83**	2Ø6 mm (56.55)	CFRP	275	/	/	/	Ø6 @ 120 mm
CFB2	**1.24**	3Ø6 mm (84.82)	CFRP	275	/	/	/	Ø6 @ 80 mm
CFB3	**1.65**	4Ø6 mm (113.09)	CFRP	275	/	/	/	Ø6 @ 60 mm
CFB4	**2.06**	5Ø6 mm (141.37)	CFRP	275	/	/	/	Ø6 @ 50 mm
DCFB1	**0.77**	2Ø6 mm (56.55)	CFRP	275	2Ø6 mm (56.55)	CFRP	20	Ø6 @ 120 mm
DCFB2	**1.16**	3Ø6 mm (84.82)	CFRP	275	2Ø6 mm (56.55)	CFRP	20	Ø6 @ 80 mm
DCFB3	**1.55**	4Ø6 mm (113.09)	CFRP	275	2Ø6 mm (56.55)	CFRP	20	Ø6 @ 60 mm
DCFB4	**1.93**	5Ø6 mm (141.37)	CFRP	275	2Ø6 mm (56.55)	CFRP	20	Ø6 @ 50 mm
SB1	**0.3**	2Ø12 mm +2Ø10 mm (383.26)	Steel	275	/	/	/	Ø6 @ 120 mm
SB2	**0.4**	4Ø12 mm +2Ø6 mm (508.92)	Steel	270.56	/	/	/	Ø6 @ 80 mm
SB3	**0.49**	4Ø12 mm +2Ø10 mm (609.45)	Steel	264.7	/	/	/	Ø6 @ 60 mm
SB4	**0.55**	6Ø12 mm (678.56)	Steel	261.7	/	/	/	Ø6 @ 50 mm

* A_r/A_{rb} is the ratio of (CFRP or steel) reinforcement area to the balanced reinforcement area.

Table 2 Mixture proportions and compressive test of cylinders for Trial mix 4.

Material	Trial Mix 4 (Designed)	Tested at 28 days		
Cement (kg)	495	Compressive strength (MPa) 100x200mm cylinder test		
Silica fume (kg) [Silica/Cement %]	79 [16%]			
Water (Liter)	149	59.02 MPa	57.92 MPa	65.45 MPa
HRWRA (Glenium 51) (Liter)	7.9	Average (MPa)		
Air content %	2	60.8 (MPa)		
Coarse Aggregate-12.5mm (kg)	990	According to ASTM C39		
Fine Aggregate (kg) [$\frac{FA}{(FA+CA)}x100\%$]	644 [39%]			
w/cm	0.26			

Table 3 Experimental values of the compressive strength. (At the age that the beams were tested)

Cube & Cylinder Test		SB group			CFB group			DCFB group		
f_{cu} 6.8 kN/sec	kN	1508.9	1414.8	1404.2	1658.5	1528.4	1636.0	1509.3	1492.9	1635.5
	MPa	67.06	62.88	62.41	73.71	67.93	72.71	67.08	66.35	72.69
	Average	64.12			71.45			68.71		
f_c' 2.4 kN/sec	kN	448.5	444.6	438.9	429.9	511.3	476.7	439.8	464.9	457.5	426.9	497.7	459.9
	MPa	57.12	56.62	55.89	54.75	65.11	60.71	56.01	59.21	58.26	54.36	63.38	58.57
	Average	56.10			60.26			58.64		
f_c' / f_{cu}		0.87			0.84			0.85		

Table 4 Experimental values for the tensile strength

Cylinder & Prism Test		SB group			CFB group			DCFB group		
f_{sp}' 0.94 kN/sec	kN	145.79	124.43	140.77	103.37	210.21	151.70	138.75	171.56	138.57
	MPa	4.64	3.96	4.48	3.29	6.69	4.83	4.42	5.46	4.41
	Average	4.36			4.94			4.76		
f_r' 0.2 kN/sec	kN	22.43	24.57	23.07	26.40	24.93	24.77	25.43	21.07	28.73
	MPa	6.73	7.37	6.92	7.92	7.48	7.43	7.63	6.32	8.62
	Average	7.01			7.61			7.52		
f_{sp}' / f_r'		0.62			0.65			0.63		

Fig.5 Two strain gauges for tested cylinder

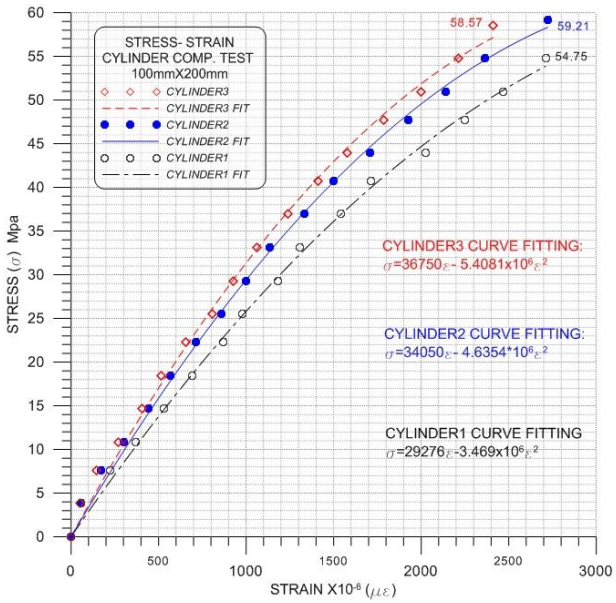

Fig. 6 Experimental Stress-Strain curve

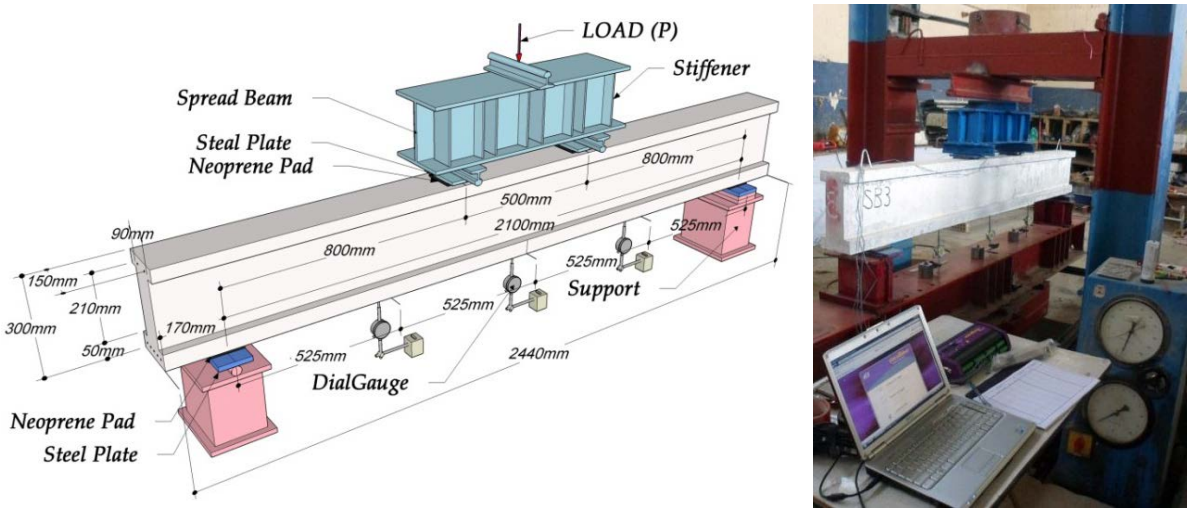

Fig. 7 Test set-up and dimensions.

Table 5 Experimental load capacities (P_{exp}) of the tested I-beams

CFB group (P_{exp} kN)				DCFB group (P_{exp} kN)				SB group (P_{exp} kN)			
CFB1	**CFB2**	**CFB3**	**CFB4**	**DCFB1**	**DCFB2**	**DCFB3**	**DCFB4**	**SB1**	**SB2**	**SB3**	**SB4**
130	155	180	170	125	150	165	195	145	215	215	220

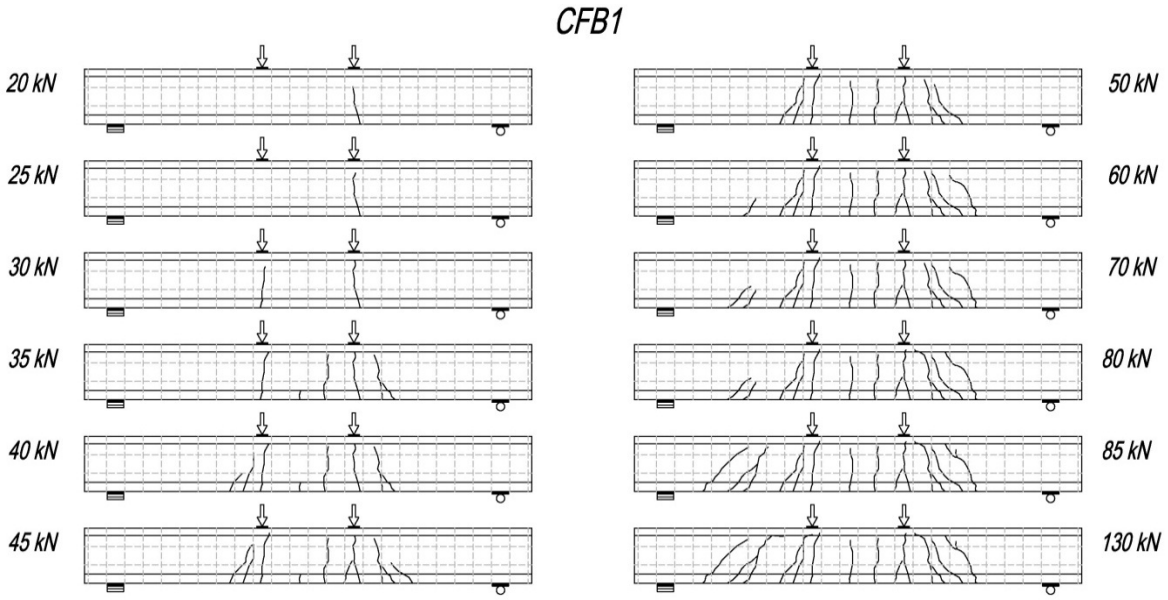

Fig. 8 Typical crack pattern (CFB1 Specimen)

Table 6 Experimental values for the service load and CFRP stress for $\sigma_c = 0.6\, f'_c$

Beam Designation	Experimental results		Service load for $\sigma_c = 0.6\, f'_c$			Corresponding tensile stress f_f		
	P_{exp} (kN)	ε_{cu} (x10^{-6})	Load $P_{s,s}$ (kN) **	ε_c (x10^{-6})	% of P_{exp}	ε_f (x10^{-6})	f_f MPa	% of f_{fu} *
CFB1	130	2240	71.8	1260	55%	11000	1793	66%
CFB2	155	2640	75.0	1260	48%	9000	1467	54%
CFB3	180	2590	91.2	1260	51%	8500	1386	51%
CFB4	170	2310	92.7	1260	55%	6200	1010	37%
DCFB1	125	2230	60.3	1152	48%	10000	1630	60%
DCFB2	150	2530	76.0	1152	51%	8000	1304	48%
DCFB3	165	2370	80.0	1152	48%	8700	1418	52%
DCFB4	195	2420	101.3	1152	52%	7000	1141	42%
SB1	145	2370	123.6	1333	85%	3800	500	/
SB2	215	2430	139.2	1333	65%	3200	500	/
SB3	215	2480	145.0	1333	67%	3000	500	/
SB4	220	2370	161.1	1333	73%	2800	500	/

* $f_{fu} = 2704\ MPa\ (Aslan\ 200\ CFRP\ rebar)$.

** $(P_{s,s}\ kN)$: Experimental values for the service load for maximum concrete stresses.

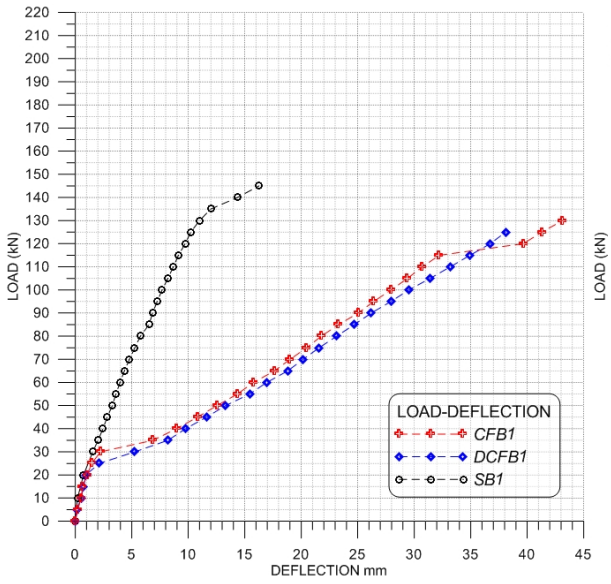

Fig. 9 Load-Deflection (Series 1)

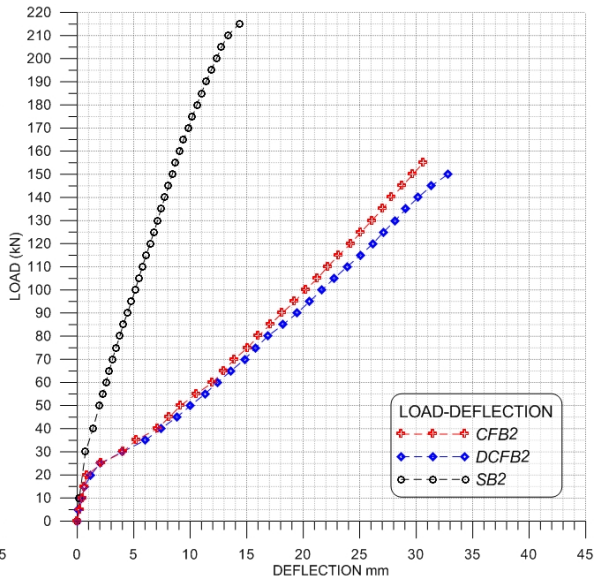

Fig. 10 Load-Deflection (Series 2)

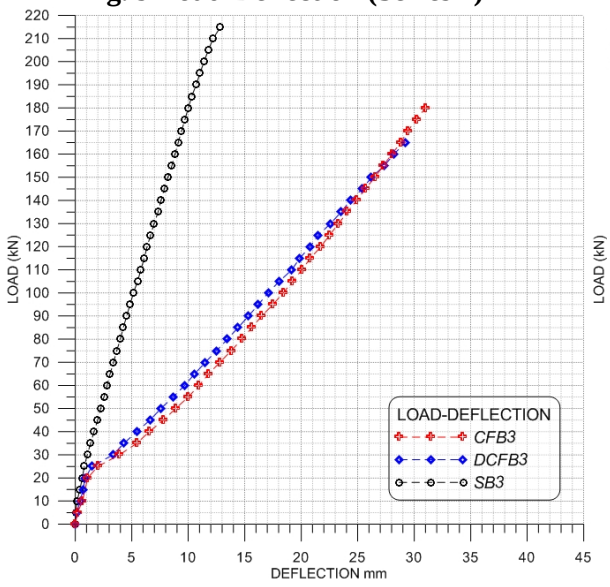

Fig. 11 Load-Deflection (Series 3)

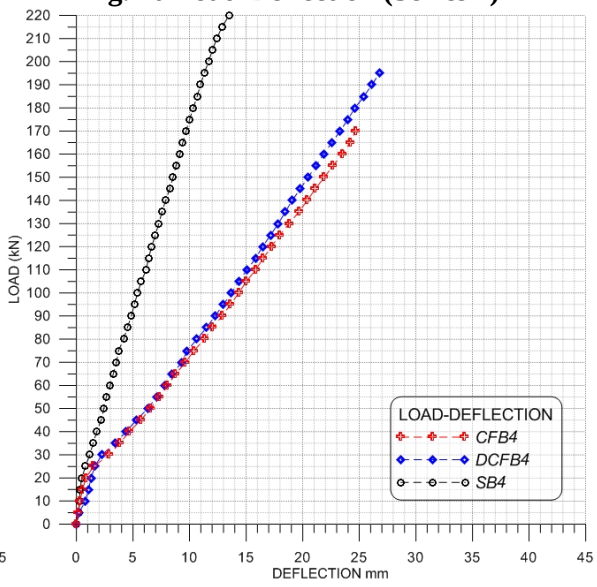

Fig. 12 Load-Deflection (Series 4)

Table 7 Experimental load at which the instantaneous deflection equals to $l/240$=2100/240=8.75mm

Group	CFB group				DCFB group				SB group			
Beam Designation	CFB1	CFB2	CFB3	CFB4	DCFB1	DCFB2	DCFB3	DCFB4	SB1	SB2	SB3	SB4
(P_{exp} kN)	130	155	180	170	125	150	165	195	145	215	215	220
($P_{s,d}$ kN) $\delta = 8.75$ mm	39.5	48.0	49.4	64.8	36.7	44.8	55.5	66.7	110.8	155.6	158.6	154
% $P_{s,d}/P_{exp}$	30%	31%	27%	38%	29%	30%	34%	34%	76%	72%	74%	70%

* ($P_{s,d}$ kN): Experimental values for the service load for maximum permissible deflection

Table 8 Experimental load at which the max. crack width equal to 0.7 mm (CFRP) & 0.4 mm (Steel)

Group	CFB group				DCFB group				SB group			
Beam Designation	CFB1	CFB2	CFB3	CFB4	DCFB1	DCFB2	DCFB3	DCFB4	SB1	SB2	SB3	SB4
(P_{exp} kN)	130	155	180	170	125	150	165	195	145	215	215	220
($P_{s,c}$ kN) w=0.7 mm (CFRP) w=0.4 mm (Steel)	35	65	95	>170	45	55	>165	185	>145	>215	>215	>220
% $P_{s,c}/P_{exp}$	27%	42%	53%	100%	36%	37%	100%	95%	100%	100%	100%	100%

* ($P_{s,c}$ kN): Experimental values for the service load for maximum permissible crack width

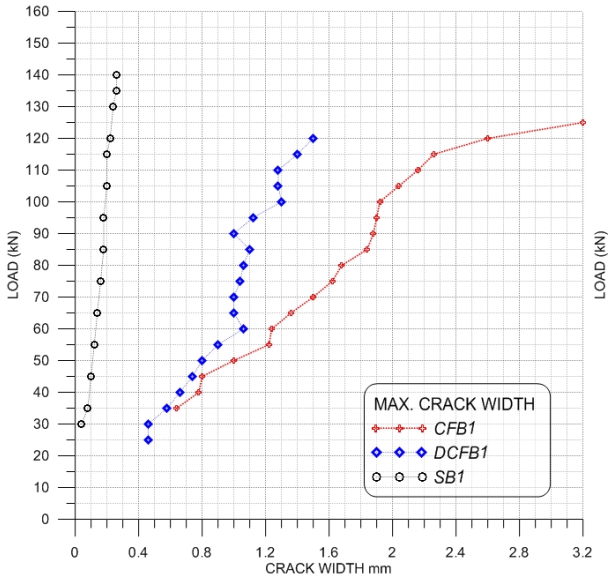

Fig. 13 Crack width evolution (Series 1)

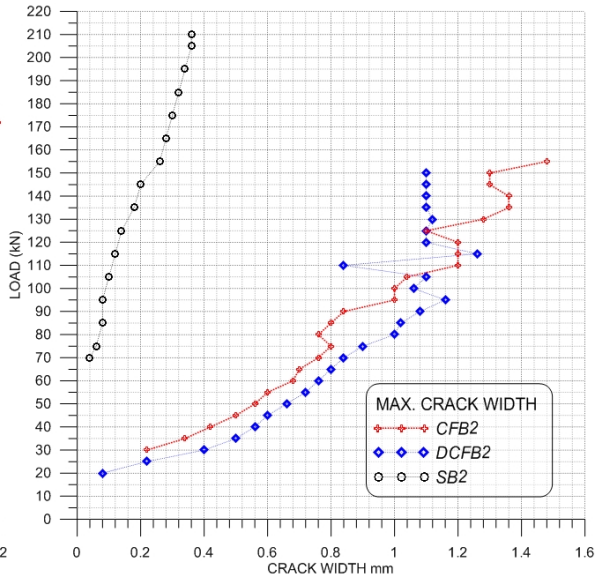

Fig. 14 Crack width evolution (Series 2)

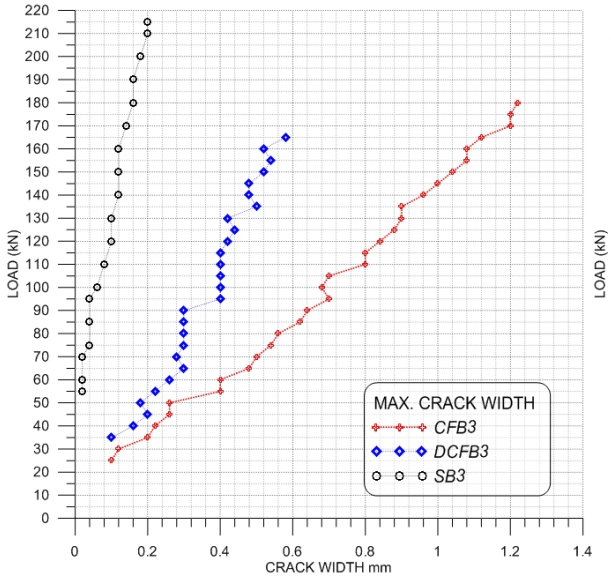

Fig. 15 Crack width evolution (Series 3)

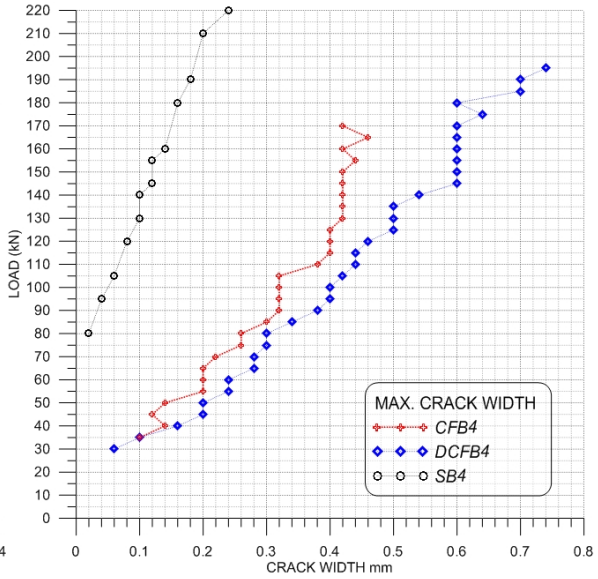

Fig. 16 Crack width evolution (Series 4)

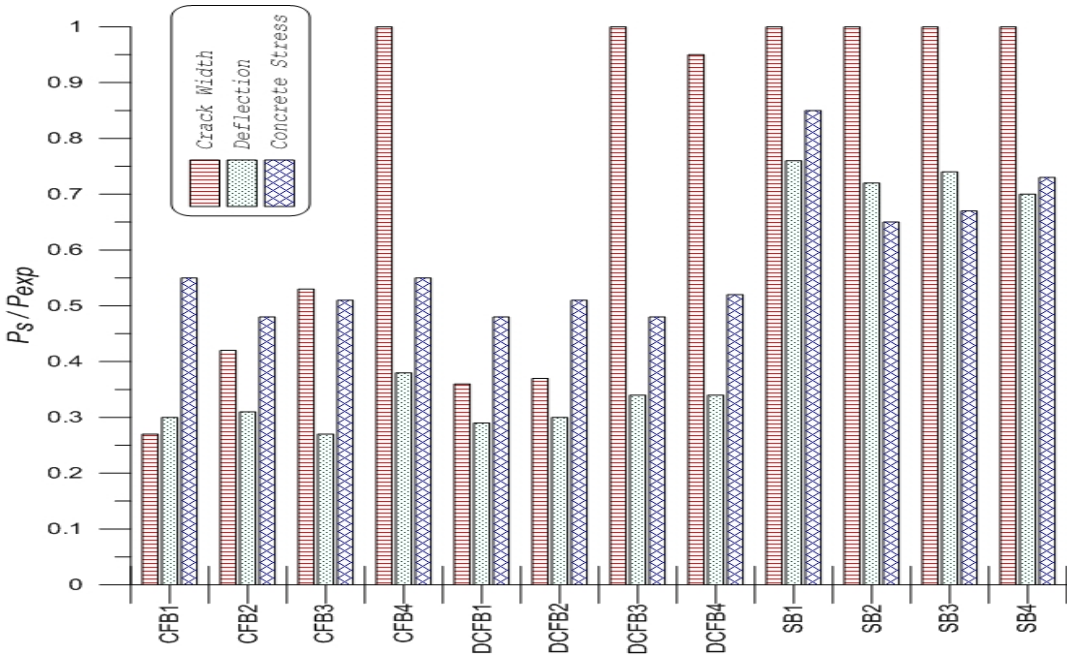

Fig. 17 Experimental service load related to the experimental failure load

Table 9 Service load P_s for each SLS

Group	CFB group				DCFB group				SB group			
Beam Designation	CFB1	CFB2	CFB3	CFB4	DCFB1	DCFB2	DCFB3	DCFB4	SB1	SB2	SB3	SB4
(P_{exp} kN)	130	155	180	170	125	150	165	195	145	215	215	220
($P_{s,d}$ kN) $\delta = 8.75\ mm$	39.5	48.0	49.4	64.8	36.7	44.8	55.5	66.7	110.8	155.6	158.6	154
% $P_{s,d}/P_{exp}$	30%	31%	27%	38%	29%	30%	34%	34%	76%	72%	74%	70%
Load $P_{s,s}$ (kN)	71.8	75	91.2	92.7	60.3	76	80	101.3	123.6	139.2	145	161.1
% $P_{s,s}/P_{exp}$	55%	48%	51%	55%	48%	51%	48%	52%	85%	65%	67%	73%
($P_{s,c}$ kN) w=0.7 mm (CFRP) w=0.4 mm (Steel)	35	65	95	>170	45	55	>165	185	>145	>215	>215	>220
% $P_{s,c}/P_{exp}$	27%	42%	53%	100%	36%	37%	100%	95%	100%	100%	100%	100%
(P_s kN)	35.0	480	49.4	64.8	36.7	44.8	55.5	66.7	110.8	139.2	145	154
% P_s/P_{exp}	27%	31%	27%	38%	29%	30%	34%	34%	76%	65%	67%	70%